Proceedings of
11th European Conference on Turbomachinery Fluid dynamics & Thermodynamics
ETC11, March 23-27, 2015, Madrid, Spain

FILM COOLING EFFECTIVENESS MEASUREMENTS ON ENGINE REPRESENTATIVE TRAILING EDGE SLOTS INCLUDING CUTBACK SURFACE PROTUBERANCES

T.H. Wong[1] - P.T. Ireland[1] - K.P. Self[2]

[1]Department of Engineering Science, University of Oxford, Oxford OX1 3PJ, United Kingdom, holt.wong@eng.ox.ac.uk, peter.ireland@eng.ox.ac.uk
[2]Rolls-Royce plc., Bristol BS34 7QE, United Kingdom, kevin.self@rolls-royce.com

ABSTRACT

The trailing edge of the high pressure turbine blade presents significant challenges to the turbine cooling engineer. The current research has focused specifically on the effect of cutback surface protuberance, or "land", shapes on film cooling effectiveness. A set of six different land geometries has been investigated in a large scale model of the trailing edge pressure side ejection slot exit. Slot height and width and lip height was maintained. Pressure sensitive paint was used to measure adiabatic film cooling effectiveness at five blowing ratios ranging from 0.6 to 1.4 in increments of 0.2. High resolution 2D distributions of film cooling effectiveness both on the cutback surface and the top of the lands were recorded.

NOMENCLATURE

A	Area (m^2)
h	Slot height (mm)
I	Intensity image
$\dot{m}$	Mass flow rate (kg/s)
M	Blowing ratio
MFC	Mass flow controller
MIX_N	Sturgess geometric parameter
$\dot{M}$	Molecular flow rate (kmol/s)
MW	Molecular weight (kg/kmol)
n	Mole fraction of Oxygen
p	Pressure (Pa)
$p(O_2)$	Partial pressure of Oxygen (Pa)
Re	Reynolds number
t	Lip thickness (mm)
u	Velocity (m/s)
w	Slot width (mm)
x	Distance from slot exit (mm)
x_p	Potential core length (mm)
y	Distance from cutback surface (mm)
z	Distance from centreline (mm)
ρ	Density (kg/m^3)
η	Adiabatic film cooling effectiveness

Subscripts

air	Air only coolant
atm	Ambient conditions
c	Coolant
dark	Lights off
m	Mainstream
mix	Mixed air-N_2 coolant
ref	Reference conditions
s	Static
surf	Painted surface

INTRODUCTION

In order to increase the fuel efficiency of civil turbofan engines, manufacturers have continued to increase the operating temperatures and pressures of new engine designs. Current designs feature high pressure turbine entry temperatures that far exceed the blade material melting point and thus require the use of air cooling to maintain an acceptable metal temperature and component life. Typically, blade cooling is accomplished through a mixture of internal cooling to reduce the metal temperature from within, and external film cooling to shield the exterior surface from the hot mainstream gas.

A particularly challenging part of the high pressure blade is the trailing edge. This section endures very high temperatures and mechanical stresses but aerodynamic efficiency requirements dictate that it must be tapered to the end with minimal thickness. The thin profile makes it difficult to feed directly with coolant internally and necessitates the use of film cooling. A common method

of film cooling the trailing edge is to position film cooling holes or slots just upstream of the trailing edge on the pressure surface side of the blade. Modern designs may include a cutback region where material is removed from the pressure surface between the film hole exits and the trailing edge to allow the coolant to exit almost tangentially to the mainstream and also reduce the risk of blockage. Cooling slots have an advantage over cooling holes in that the film is uniform along the spanwise width which provides even surface coverage and the Coanda effect causes the film to stick to the surface more readily rather than lifting off into the mainstream gas (Sargison 2001). However, continuous cooling slots are not mechanically robust as the slot weakens the design. This makes them poorly suited to areas which undergo severe mechanical and thermal stresses like the blade trailing edge. These considerations cause designers to use interrupted cooling slots which have an internal "bridge" connecting the two sides and dividing the continuous slot into discrete slots, as well as an external protuberance, or "land", which extends from the bridge to the trailing edge, dividing and stiffening the cutback area. An example of a pressure surface slot cooling design is shown in Figure 1.

There have been many studies investigating general film cooling slots experimentally. Goldstein (1971) provided a review of much relevant work up to that year on various slot designs including tangential and angled slots. Kacker and Whitelaw (1967) showed that the effect of mainstream boundary layer thickness on adiabatic film effectiveness is small. Mukherjee (1976) performed a literature survey to form a number of correlations for predicting film effectiveness and the length of the initial "potential core" region of unity effectiveness. Sturgess (1986) and Sturgess and Pfeifer (1986) investigated the film cooling of practical combustor slots. They formed a geometric parameter, MIX_N, for characterising practical combustor slot geometries and reported the relation between potential core length, blowing ratio, and MIX_N.

Several studies have focused on slots applied to the turbine blade trailing edge. Taslim et al. (1992) studied the film cooling effectiveness on the cutback surface downstream of the slot with straight bridges and lands dividing the slots. They varied injection angle, lip thickness to slot height ratio t/h, slot width to slot height ratio w/h, blowing ratio and density ratio. Martini et al. (2005) investigated how three different slot designs used in modern blades affect the film cooling effectiveness, heat transfer coefficients and discharge coefficients in the near slot region of the cutback. These geometries featured different internal slot geometries but no external lands on the cutback surface. Murata et al. (2012) used the transient infrared thermography method to compare four different slot geometries for film cooling effectiveness and heat transfer coefficients. Two of these featured plain slots with straight lands and tapered lands respectively. Yang and Hu (2011) and Yang and Hu (2012) used stereoscopic particle image velocimetry to take flow field measurements of an interrupted slot geometry with and without tapered diffuser lands and compared these with film cooling effectiveness maps acquired using the pressure sensitive paint (PSP) technique. Ling et al. (2015) used an MRI technique to take velocity field and film effectiveness measurements using tapered straight and diffuser lands.

To the best of the authors' knowledge, there has been little detailed study in the open literature focusing on the effect of land shapes on film cooling effectiveness, both on the cutback surface after the slot and on top of the lands themselves. The scope of the current work is to provide a set of experimental data with detailed film cooling effectiveness maps for six different land shapes similar to modern blade designs.

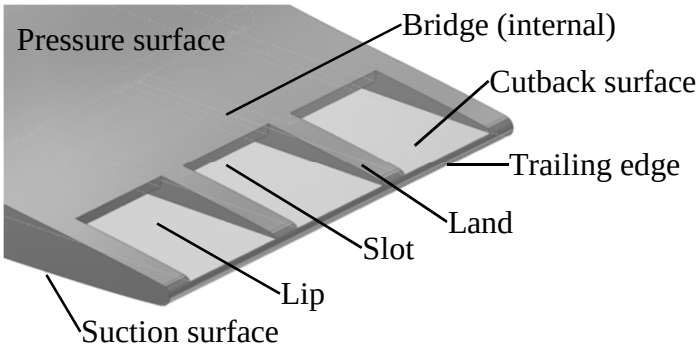

Figure 1. Basic trailing edge pressure surface slot cooling design

EXPERIMENTAL SETUP

The experiments were conducted in one of the low speed facilities of the Osney Thermo-Fluids Laboratory, University of Oxford. A large scale model of a portion of the trailing edge pressure side slot and cutback was manufactured. A schematic of the wind tunnel is shown in Figure 2. Detailed cross-sectional plan and side views of the test section are shown in Figure 3-a.

The mainstream flow was ambient air drawn in through the open intake by a water ring vacuum pump. The air passed through an air filter at the intake, a flow restriction and a settling section before entering the test section. The settling section was sufficiently long to reduce any influence of the inlet restrictions on the velocity profile at the test section. Following the test section, the mixed flow entered an outlet plenum before exiting through five hoses. The hoses combined into a single long pipe with an orifice plate for mass flow measurement and a valve for mass flow control before going to the vacuum pump.

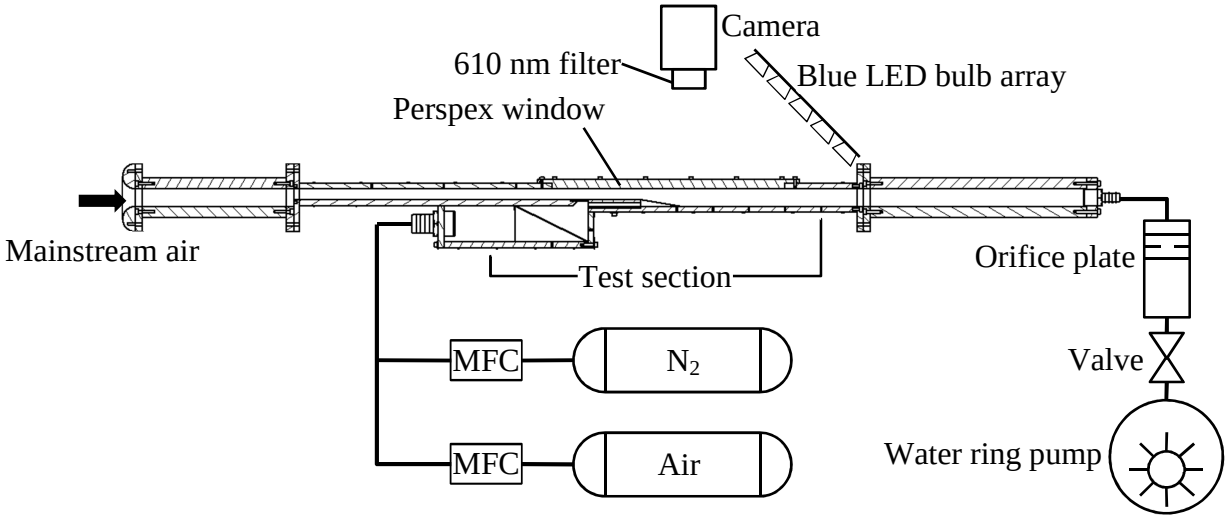

Figure 2. Wind tunnel schematic

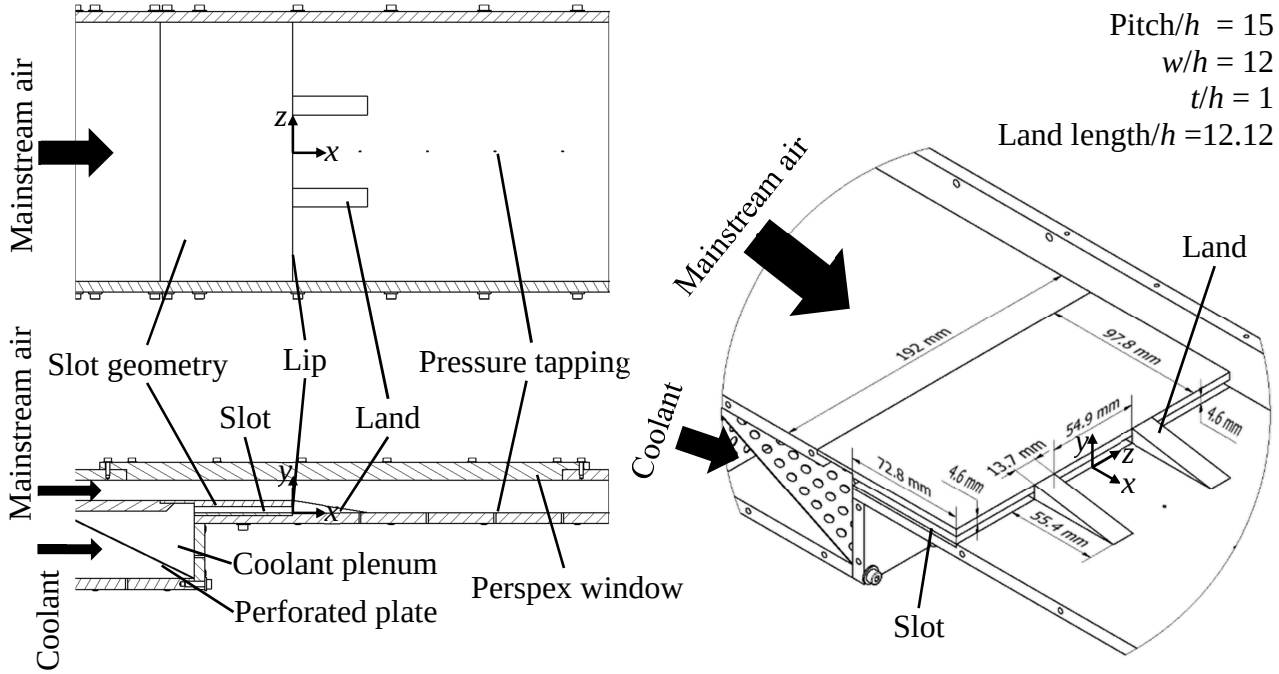

(a) Cross-sectional views (b) Dimensions

Figure 3. Detailed views of test section

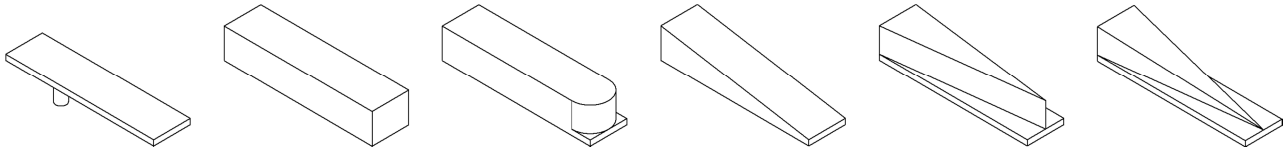

(a) No land (b) Block (c) Rounded (d) Tapered (e) Diffuser (f) Tapered diffuser

Figure 4. Land geometries

The coolant flow was made up of a mixture of air from the 689 kPa laboratory compressed air supply and Nitrogen from a compressed Nitrogen bottle, both at ambient temperature. The coolant air-Nitrogen ratio and flow rate were controlled by two automatic mass flow controllers, one for each source. The two streams were mixed in a hose manifold system before entering the coolant plenum, which contained a perforated plate to dissipate the jets from the hose inlets. The coolant then passed through the slot and onto the test plate where it mixed with the mainstream flow.

The permanent portion of the test section was made from stainless steel. The removable Perspex window was positioned above the test plate and slot to allow for easy removal of the slot geometry and lands while also allowing full optical access. The slot geometry was manufactured using stereolithography as a plain rectangular slot divided into three by bridges and lands with dimensions as shown in Figure 3-b. Three slots were included so that any lateral effects due to the boundary layers of the test section walls would not significantly affect the central slot where the measurements were taken. The test plate and lands were made from aluminium and removable to allow painting and testing of different land geometries. The six land geometries tested are shown in Figure 4. Except for the "no land" configuration, they all have the same height, width and depth.

Measurement Technique

The UniFIB PSP used contained a blend of Fluoro/Isopropyl/Butyl polymer (FIB), Platinum Tetra(Pentafluorophyenyl)Porphine (PtTFPP) and white pigment. PtTFPP is a luminophore which is sensitive to Oxygen. FIB is a gas-permeable polymer binder used to suspend the luminophore on the painted surface while allowing Oxygen molecules to diffuse into the polymer and interact with the luminophore. When exposed to light of a wavelength range of 380 nm to 520 nm, the luminophore molecule is excited to a higher electronic state. The molecule returns to its ground state by emitting photons with a wavelength in the range from 620 nm to 750 nm. Alternatively, the luminophore molecule can follow a non-radiative process and return to its ground state if it comes in contact with an external molecule of Oxygen. This is known as Oxygen quenching as explained by Quinn et al. (2013). The intensity of the emitted light reduces with an increase in partial pressure of Oxygen in contact with the painted surface. This feature can be used to measure the partial pressure of Oxygen at all points on the painted surface. If the concentration of Oxygen in the fluid is known, then the absolute pressure on the surface can be found. Alternatively, if two streams of fluid with different, known concentrations are used, then PSP can be used to determine the proportions of the two streams present in the mixed gas at any particular location. In the case of a film cooled surface, the adiabatic film cooling effectiveness can be calculated using the mass transfer analogy as explained by Han and Rallabandi (2010). A comparison between the PSP technique and the thermochromic liquid crystal technique for measuring film cooling effectiveness can be found in Caciolli et al. (2013).

In the present research, the test plate and lands were painted with UniFIB by airbrushing and illuminated by a grid of 12 blue LED lamps at a wavelength of approximately 470 nm. The intensity images were taken using an AVT Bigeye G-283B Cool monochrome CCD camera with a 610 nm long pass filter at a resolution of 1928 x 1452 pixels. The entire test section, lights and camera were surrounded by black sheets to maintain as dark an environment as possible and reduce PSP degradation over time. In order to reduce the effects of noise in the image, 30 frames were taken for every experimental condition and each pixel was averaged over the 30 frames to create the intensity

images used for post processing. A dark image was also taken with the blue LEDs turned off to take into account any remaining ambient light and sensor inconsistencies.

Calibration

The PSP was calibrated in-situ by taking 11 intensity images at known partial pressures of Oxygen I_{mix}, 11 corresponding reference intensity images at ambient conditions I_{ref}, and 1 dark image I_{dark}. The partial pressure was set by flushing the test section with a steady mixture of air and Nitrogen at known mass flow rates. The mass flow rate was kept low, at only several g/s and maintained for a few minutes to ensure full coverage without significant local pressure variations. The absolute pressure on the painted surface $p_{s\,surf}$, was measured using a static pressure tapping on the surface. The ambient pressure p_{atm}, was measured using a mercury barometer situated nearby.

Air and Nitrogen have known molecular weights, MW_{air} = 28.95 kg/kmol and MW_{N2} = 28.01 kg/kmol respectively. The molecular flow rate of the air and Nitrogen streams at each calibration point was calculated using equation 1. The two streams were mixed before entering the test section and the mole fraction of Oxygen in the combined air and Nitrogen mixture n_{mix}, was calculated using equation 2, where the mole fraction of Oxygen in the air stream n_{air} = 20.95%. The partial pressure of Oxygen on the painted surface $p(O_2)_{surf}$, was calculated by multiplying with the measured surface pressure from the pressure tappings using equation 3. The partial pressure of Oxygen under reference (ambient) conditions $p(O_2)_{ref}$, was simply the ambient pressure multiplied by the mole fraction of Oxygen in air, equation 4. The ratio of intensities was adjusted for dark as in equation 5 and averaged over the entire investigated area to give 11 mean values of intensity ratio, I_{ratio}. This was then plotted against the ratio of the two partial pressures, $p(O_2)_{surf}/p(O_2)_{ref}$ to create a mean calibration curve shown in Figure 5. An alternate calibration curve using only a 400 pixels square sample around the pressure tapping was also created and found to be practically identical, showing that there was no significant non-uniformity over the investigated area.

$$\dot{M} = \frac{\dot{m}}{MW} \tag{1}$$

$$n_{mix} = n_{air} \times \frac{\dot{M}_{air}}{\dot{M}_{air} + \dot{M}_{N_2}} \tag{2}$$

$$p(O_2)_{surf} = n_{mix} \times p_{s\,surf} \tag{3}$$

$$p(O_2)_{ref} = n_{air} \times p_{atm} \tag{4}$$

$$I_{ratio} = \frac{I_{ref} - I_{dark}}{I_{mix} - I_{dark}} \tag{5}$$

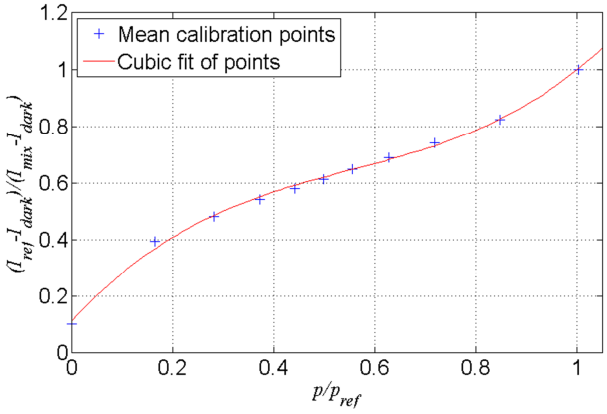

Figure 5. PSP calibration curve

The film cooling effectiveness measurements were taken by running the experiment twice for each geometry at each blowing ratio. Once using Nitrogen as the coolant, and once using air as the coolant. Intensity images were taken at each condition just as in the calibration and converted to values of $p(O_2)_{surf}/p(O_2)_{ref}$ for each pixel with Nitrogen and with air as the coolant. This was related to film effectiveness by equation 6 as shown by Han and Rallabandi (2010) where the coolant gas has a similar molecular weight as air.

$$\eta \approx 1 - \frac{p(O_2)_{surf,N_2}/p(O_2)_{ref}}{p(O_2)_{surf,air}/p(O_2)_{ref}} \tag{6}$$

Operating Conditions

The total exit flow including both mainstream and coolant gas was set at 31 g/s and the blowing

ratio was set by adjusting the mass flow ratio between the mainstream and coolant streams using the mass flow controllers. Mainstream air was at ambient conditions of approximately 293 K, 101 kPa, with a mean flow velocity between 6.6 and 7.8 m/s (calculated from the measured mainstream mass flow rate, density and area). Coolant gas was also at ambient temperature, giving a density ratio of approximately 1. The coolant stream velocity varied from 4.8 to 9.6 m/s depending on the blowing ratio. The Reynolds number of the coolant stream Re_c, based on the slot height, varied from 1400 to 3000. Blowing ratio M, was defined as in equation 7 and in this study varied from 0.6 to 1.4 in increments of 0.2.

$$M = \frac{\rho_c u_c}{\rho_m u_m} = \frac{\dot{m}_c A_{inlet}}{A_{slot} \dot{m}_m} \tag{7}$$

Uncertainties and Limitations

To ensure as consistent lighting as possible, the position and intensity of the lighting was not changed throughout the calibration and tests. The camera aperture and exposure was set such that the majority of the sensor's intensity range was used without causing saturation at any local point. Maximum local intensity was over 90% and maximum mean intensity was over 60% for zero p/p_{ref}. Calibration showed a maximum deviation of recorded data from the cubic fit curve to be less than 3%. Since there is some drift of calibration drift over time, it was ensured that the calibration curve used for tests was not older than 10 days. Following the perturbation method of Moffat (1988), the greatest uncertainty in film effectiveness measurements is at lower effectiveness when the difference in intensity between the reference and test images is smaller. For $\eta < 0.2$, uncertainty > 0.071 and for $\eta > 0.8$, uncertainty < 0.015. Blowing ratio uncertainty was calculated to be ≈ 9%.

In order to take into account temperature effects on the response of the PSP, a gas thermocouple was used to measure the coolant temperature just before entry into the slot. Han and Rallabandi (2010) showed that the temperature effects could be reduced by ensuring that a reference image is taken at the same temperature as each test image during calibration and during the experiments. By monitoring the coolant temperature and taking a separate reference image immediately after each test image, the temperature effects were minimised for the current study.

The density ratio used in the current study was different to a typical real engine density ratio of over 2. However, relative effectiveness comparisons between the different geometries in the current study as well as other studies conducted at similar density ratios is still possible and the data forms a basis for co-validation with numerical simulations in the future.

RESULTS AND DISCUSSION

The PSP technique allows high resolution 2D adiabatic film effectiveness measurements over the cutback surface and top of the lands to be made. Figure 8 shows some of the 2D plots taken in the current study. All of the figures correspond to a plan view of the cutback region and lands with the slot exit and lip aligned with the top border of the plots, i.e. where $x/h = 0$. The centreline is at the midpoint between the lands where $z/h = 0$. Measurements were taken for M = 0.6, 0.8, 1.0, 1.2 and 1.4, but only M = 0.6, 1.0 and 1.4 are shown here for brevity. Blue regions show poor coverage from the Nitrogen coolant and correspond to low film cooling effectiveness and red regions correspond to high effectiveness.

From Figure 8-b to f, it can be seen that film cooling effectiveness is very low on top of the lands, not exceeding 0.2 along the centre of the land. This shows that very little coolant is able to wash over the lands. Figure 6 shows a close-up view of the right hand land in Figure 8-d1, where the lands are tapered down to meet the cutback surface. There is a small increase in effectiveness apparent along the edges of the lands, an effect more apparent at low M. Otherwise, the mainstream air appears to stick to the land surface all the way to the end, preventing the coolant air from having any significant effect over the lands. Geometry (a) with no lands actually has better film cooling

effectiveness in the gap region where the lands would be, as the recirculation region encourages the coolant flow to enter the gap. Yang and Hu (2011) showed 2D plots of film cooling effectiveness using a "no land" geometry similar to geometry (a) and a tapered diffuser geometry similar to geometry (f). They used the same $t/h = 1$, but a much smaller $w/h = 2$ compared to the current study's $w/h = 12$. Their report showed a similar result for the "no land" geometry, with the coolant flow able to spread into the gap region. However, their report for the tapered diffuser geometry showed significantly higher film effectiveness on top of the lands, as much as 0.4 near the lip and 0.7 towards the end. This discrepancy could be due to the difference in Re_c ($Re_c = 2800$ for Yang and Hu (2011) and $Re_c = 1400$-3000 for current study) and also w/h used in the two studies. Their stereoscopic PIV measurements identified the vortices originating from the corners of the slot channels as the main factor encouraging coolant flow to wash over the top of the lands, especially when $M < 1.0$. The proximity of the two corners of the slot channels may be a factor in determining how the vortices form and to what extent they encourage flow to wash over the lands, although no 3D or unsteady flow data was taken in the current study to confirm this. Murata et al. (2012) reported 2D effectiveness measurements taken over the top of the lands for straight and diffuser lands using $w/h = 4.6$. They found very low effectiveness down the length of the lands, not exceeding 0.25 along the centre, with higher effectiveness along the edges. Ling et al. (2015) used an MRI technique to take 2D effectiveness measurements over the top of the lands for straight and diffuser lands using $w/h = 3$. They also found very low effectiveness on top of the lands for the straight and weakly diffused lands, not exceeding 0.2 along the centre. Both of these reports are in agreement with the current study. However, Ling et al. (2015) also tested a strongly diffused land with a high diffusion angle and tapering which showed some effectiveness up to 0.4 near the start of the lands. They theorised that this was due to the strong tapering of the land in that case, rather than the diffusion, which caused flow separation at the start of the lands leading to greater coolant mixing and higher effectiveness in that region. This bears some similarity in shape and results to the tapered diffuser geometry used by Yang and Hu (2011) and may also be related to the relatively low w/h used in both studies.

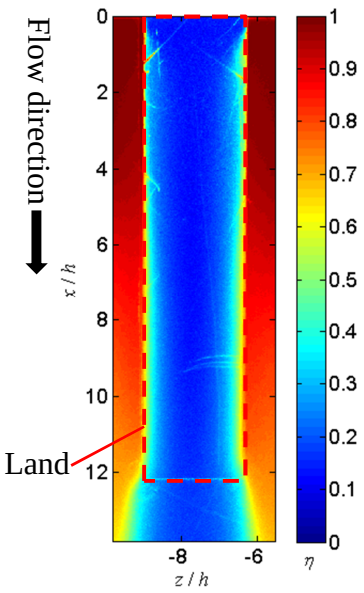

Figure 6. Close-up view of tapered land

Regions of low film effectiveness are distinctly visible downstream of the lands (bridges in the case of geometry (a)) where mainstream air is drawn in to the gap to mix with the coolant. For the tapered geometries (d) and (f), the region of low effectiveness is larger and more pronounced than the corresponding non-tapered equivalents, geometries (b) and (e) respectively. This is due to the tapered land surface creating a ramp for the mainstream air to follow down to the cutback surface, discouraging mixing of the mainstream and coolant flows. The non-tapered lands, on the other hand, create a sudden gap which encourages the coolant flow to spread.

Figure 9 shows spanwise averaged film cooling effectiveness for each geometry. The "lands included" plots in the left hand column take an average of the region in between the centre-points of the two lands. The "centreline" plots in the right hand column include only a 100 pixel (8.43 mm) wide strip down the centre of the cutback region extending downstream from the slot. The position of the end of the lands is marked in the plots.

Considering only the centreline effectiveness, all geometries show a similar overall picture, with initial unity effectiveness for some distance, called the "potential core" length x_p, before decaying. In the current study, x_p/h was determined by plotting the natural logarithm of the centreline effectiveness against the natural logarithm of x/h and taking a straight-line extrapolation through the data to the point of implied unity effectiveness. This process is illustrated in Figure 7-a using the block lands as an example. x_p/h increased with M for all geometries, as shown in Figure 7-b, to a

maximum value of 8.97. The increase in x_p/h becomes smaller as M increases, suggesting a non-linear relationship between the two. Sturgess and Pfeifer (1986) found that the potential core length to slot height ratio x_p/h, increased with M to a peak value before reducing to a plateau value at very high M. x_p/h was also found to increase with a reduction in the MIX_N parameter (where $MIX_N = 0$ corresponds to a clean slot with realistically thick lip) and t/h for the same M. No relationship between the optimum M with the largest x_p/h and MIX_N or t/h was found. The MIX_N parameter is specific to combustor slot geometries so not all the terms have a direct equivalent in a trailing edge slot. However, the current study can be approximated as a clean slot with an equivalent $MIX_N = 0$ and $t/h = 1$. Their data for $MIX_N = 0.04$ and $t/h = 0.4$, the closest available to the current study, is plotted in Figure 7-b, showing a maximum x_p/h of 6.2 for $M = 1.05$. When compared with the Sturgess and Pfeifer (1986) data, x_p/h is greater for all M, which may be due to the lower MIX_N. The current study does demonstrate the non-linear relationship between M and x_p/h but there is insufficient data for a detailed comparison and the range of M in the current study did not show a peak value in x_p/h. Taslim et al. (1992), using a clean tangential slot with $t/h = 1$, $w/h = 5$ and $Re_c = 1400\text{-}12000$, reported a linear correlation $x_p/h = 5M$ which is also plotted on Figure 7-b. This is slightly lower than the current study and could be due to the difference in Re_c and w/h used. The proximity of the lands in their study may have encouraged mainstream and coolant mixing, resulting in the shorter x_p/h compared to the current study. Predictions of x_p/h based on the correlations of Mukherjee (1976) are also plotted on Figure 7-b. The correlations take Re_c into account but are based on 2D slots without a finite slot width. These agree largely in magnitude with the current study while also being slightly higher than the data of Taslim et al. (1992). This indicates that the w/h used in the current study is sufficiently high to nearly approximate a 2D slot along the centreline. However, the correlations of Mukherjee (1976) do predict a linear relationship between x_p/h and M which is not apparent in the current study. Aside from the tapered case, the shape of the land appears to have little effect on x_p/h.

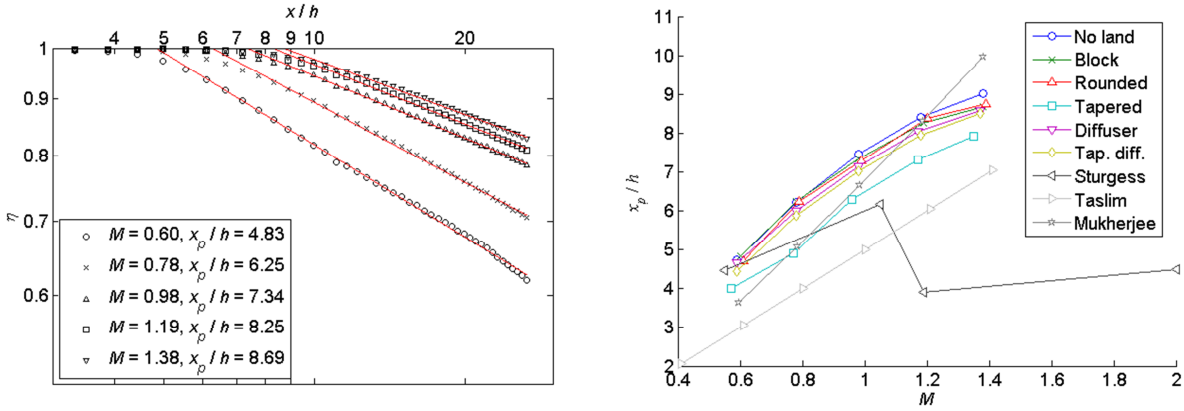

(a) Determining potential core length for block lands

(b) Potential core length at different blowing ratios

Figure 7. Potential core length

The rate at which effectiveness decreases is greater for lower M. This agrees with the trends shown by Martini et al. (2005) and Murata et al. (2012) in their film effectiveness studies. Geometry (a) with no lands showed the highest effectiveness, followed by geometries (b), (c), (e) and (f), all with very similar centreline effectiveness for all M. Geometry (d) showed the lowest effectiveness, illustrating the previously mentioned issue of the mainstream flow being pulled down by the ramped surface, encroaching into the cutback region before the end of the lands and leaving a large "hot gas" wake behind each land which also affects the central slot region.

Including the lands results in a lower spanwise average for all of the geometries, particularly up to the end of the lands. All but geometry (a) begin with an effectiveness of approximately 0.86. Geometry (a) with no lands is able to recover some effectiveness due to the coolant being able to spread into the gap where the lands would be. However, the effectiveness at the end of the lands still

reduces to 0.84 even for M = 1.4. Geometries (b) and (c) both show a sudden increase in effectiveness at the end of the lands due to the coolant spreading into the gap left but this decays quickly. The rounded geometry has a smoother jump, but overall is almost identical to the block geometry. As in the plots of centreline effectiveness, geometry (d) shows lower effectiveness, as the mainstream is pulled towards the cutback surface, encouraging mixing with the coolant, reducing effectiveness between the lands. Unlike with geometries (b) and (c), the plot does not exhibit a sudden increase in effectiveness because the mainstream air follows the land surface all the way down to the cutback surface which does not allow the coolant to spread into the gap. The diffuser geometries (e) and (f) initially show a gradual increase in average effectiveness down the length of the lands due to the coolant being allowed to spread over a larger cutback region by the land shape. This results in a peak effectiveness of 0.92 at x/h = 7.5 for M = 1.4 and 0.88 at x/h = 4.0 for M = 0.6. For M > 0.8 the effectiveness from x/h = 5 onwards is highest of all the geometries, reaching 0.89 for at the end of the lands for M = 1.4. However, for M < 0.8, the coolant flow is insufficient to fill the entire region, resulting in effectiveness at the end of the lands becoming lower than geometry (a), although still higher than the other geometries. Effectiveness after the lands is slightly lower compared to (b) and (c) since there is no recovery at the end of the lands. The tapered version of the diffuser geometry shows only a slight reduction in effectiveness overall compared to the non-tapered version.

SUMMARY AND CONCLUSIONS

Detailed distributions of adiabatic film cooling effectiveness have been measured over the cutback and land top surfaces of large scale geometries representing turbine blade trailing edges using the PSP technique. Six different land geometries were tested at five blowing ratios from 0.6 to 1.4 with a density ratio of 1. The coolant Reynolds number ranged from 1400 to 3000. The “potential core” with unity effectiveness, after which effectiveness decayed, was measured in all cases. Increasing blowing ratio increased the length of the potential core and also reduced the rate at which effectiveness decayed. With all geometries, at all blowing ratios tested, the coolant was largely unable to wash over the top surfaces of the lands, resulting in low effectiveness on the land top surface. Having no lands at all increased the spanwise averaged effectiveness since the coolant was able to spread into the gap left by the lands. In the current study, it was found that tapering the lands did not encourage coolant flow to wash over the top. Rather, it pulled the mainstream flow down to the cutback surface, creating a wake of mainstream flow after the land which the coolant flow was unable to penetrate. The diffuser geometries performed well at blowing ratios above 0.8 as the coolant was able to spread and fill out the increased cutback area, resulting in a higher spanwise average effectiveness than all other geometries, including the “no lands” geometry from approximately x/h = 5 onwards up until the end of the lands. However, at a blowing ratio of 0.6, the coolant was unable to fill the expanding cutback surface and the film decayed faster, resulting in a lower effectiveness than the “no lands” case at the end of the lands, although still better than the other geometries.

In the case of turbine blades, the end of the lands is also typically the end of the blade, so the effectiveness after that point is not of great concern. The region nearest the trailing edge is generally the hottest and most challenging part of the blade, so the effectiveness just before the end of the lands is very important. The current research has shown that, amongst the six current geometries tested, the tapered diffuser geometry provides the most favourable effectiveness, especially near the end of the lands, provided the blowing ratio is not below 0.8, in which case no lands would be preferable.

ACKNOWLEDGEMENTS

The authors would like to express their thanks to Rolls-Royce plc for supporting this research and to the technicians of the Osney Thermo-Fluids laboratory for their assistance in manufacturing and assembling the experimental apparatus.

REFERENCES

Caciolli,G., Facchini,B., Picchi,A. and Tarchi,L. (2013) *Comparison between PSP and TLC Steady State Techniques for Adiabatic Effectiveness Measurement on a Multiperforated Plate,* Experimental Thermal and Fluid Science, **48**(0) pp. 122-133.

Goldstein,R.J. (1971) *Film Cooling,* Advances in Heat Transfer, **7**(1) pp. 321-379.

Han,J. and Rallabandi,A. (2010) *Turbine Blade Film Cooling using PSP Technique,* Frontiers in Heat and Mass Transfer (FHMT), **1**(1) .

Kacker,S.C. and Whitelaw,J.H. (1967) *The Dependence of the Impervious Wall Effectiveness of a Two-Dimensional Wall-Jet on the Thickness of the Upper Lip Boundary Layer,* International Journal of Heat and Mass Transfer, **10**(11) pp. 1623-1624.

Ling,J., Elkins,C.J. and Eaton,J.K. (2015) *The Effect of Land Taper Angle on Trailing Edge Slot Film Cooling,* Journal of Turbomachinery, **137**(7) pp. 071003-071003.

Martini,P., Schulz,A. and Bauer,H. (2005) *Film Cooling Effectiveness and Heat Transfer on the Trailing Edge Cutback of Gas Turbine Airfoils with various Internal Cooling Designs,* Journal of Turbomachinery, **128**(1) pp. 196-205.

Moffat,R.J. (1988) *Describing the Uncertainties in Experimental Results,* Experimental Thermal and Fluid Science, **1**(1) pp. 3-17.

Mukherjee,D.K. (1976) *Film Cooling with Injection through Slots,* Journal of Engineering for Gas Turbines and Power, **98**(4) pp. 556-559.

Murata,A., Nishida,S., Saito,H., Iwamoto,K., Okita,Y. and Nakamata,C. (2012) *Effects of Surface Geometry on Film Cooling Performance at Airfoil Trailing Edge,* Journal of Turbomachinery, **134**(5) pp. 051033-051033.

Quinn,M.K., Gongora-Orozco,N., Kontis,K. and Ireland,P. (2013) *Application of Pressure-Sensitive Paint to Low-Speed Flow Around a U-Bend of Strong Curvature,* Experimental Thermal and Fluid Science, **48**(0) pp. 58-66.

Sargison,J.E. (2001) *Development of a Novel Film Cooling Hole Geometry,* DPhil Thesis, **University of Oxford**.

Sturgess,G.J. (1986) *Design of Combustor Cooling Slots for High Film Effectiveness: Part I—Film General Development,* Journal of Engineering for Gas Turbines and Power, **108**(2) pp. 354-360.

Sturgess,G.J. and Pfeifer,G.D. (1986) *Design of Combustor Cooling Slots for High Film Effectiveness: Part II—Film Initial Region,* Journal of Engineering for Gas Turbines and Power, **108**(2) pp. 361-369.

Taslim,M.E., Spring,S.D. and Mehlman,B.P. (1992) *Experimental Investigation of Film Cooling Effectiveness for Slots of various Exit Geometries,* Journal of Thermophysics and Heat Transfer, **6**(2) pp. 302-307.

Yang,Z. and Hu,H. (2012) *An Experimental Investigation on the Trailing Edge Cooling of Turbine Blades,* Propulsion and Power Research, **1**(1) pp. 36-47.

Yang,Z. and Hu,H. (2011) *Study of Trailing-Edge Cooling using Pressure Sensitive Paint Technique,* Journal of Propulsion and Power, **27**(3) pp. 700-709.

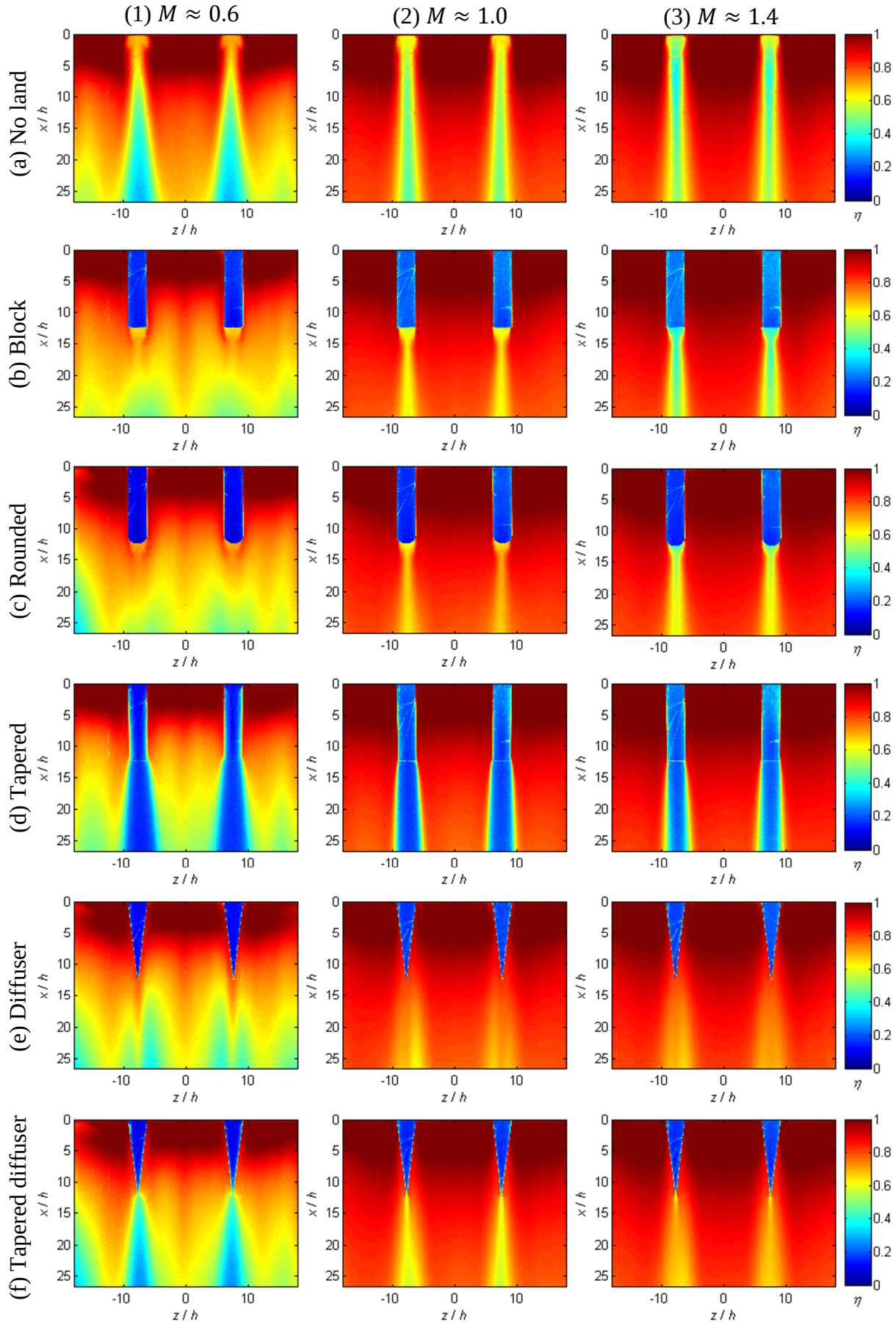

Figure 8. 2D Film cooling effectiveness at different blowing ratios (flow from top to bottom)

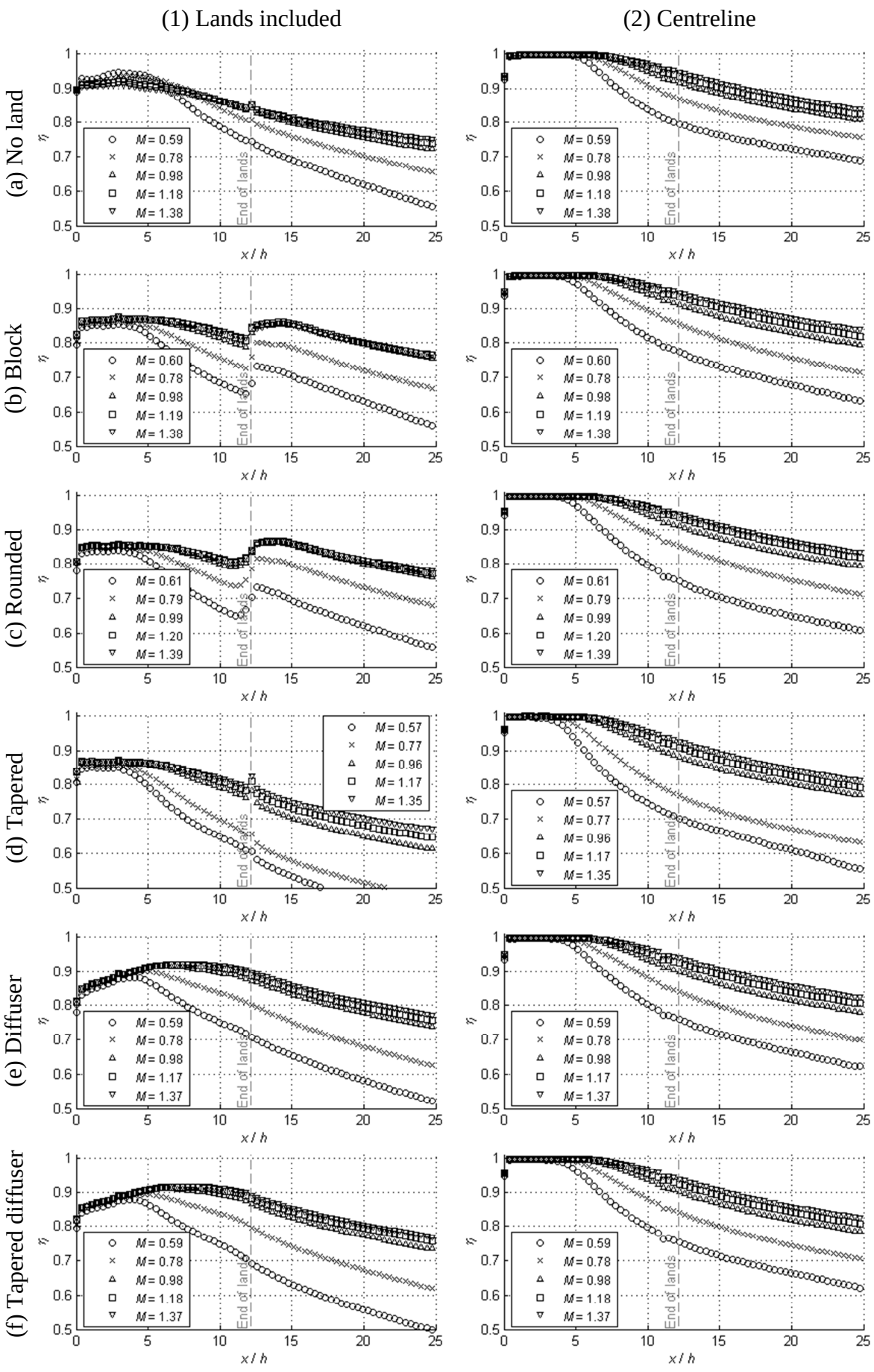

Figure 9. Spanwise average film cooling effectiveness at different blowing ratios